Striking effect of the iron stearate purity on the shape and size of maghemite nanoparticles

Sakina Meftah, Anh-Tu Ngo, Ashkan Shahmanesh, Alexa Courty, Djimédo Kondo, Fahmi Bedoui, Isabelle Lisiecki

Striking effect of the iron stearate purity on the shape and size of maghemite nanoparticles

Sakina Meftah[1,2], Anh-Tu Ngo[1], Ashkan Shahmanesh[1], Alexa Courty[1], Djimédo Kondo[3], Fahmi Bedoui[2,4], Isabelle Lisiecki[1*]

1- Sorbonne Université, CNRS, De la Molécule aux Nano-Objets: Réactivité, Interactions Spectroscopies, MONARIS, 75005 Paris, France.

2- Centre de Recherche de Royallieu, Roberval Laboratory for Mechanics, CNRS, Université de Technologie de Compiègne, 60203 Compiègne, France.

3- Sorbonne Université, CNRS, Institut Jean Le Rond D'Alembert, 75005 Paris, France.

4-California Institute of Technology, Materials and Process Simulation Center, 91106, Pasadena California.

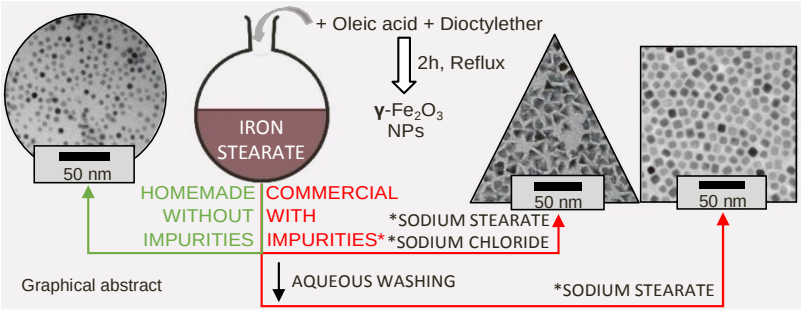

ABSTRACT

In general, the synthesis of maghemite nanoparticles (NPs) by thermal decomposition of commercially available iron stearate precursors, in the presence of oleic acid, yields spherical nanoparticles. However, we show in this article that the synthesis of NPs from commercially available precursors (Commercial grade and washed) results in the formation of uniformly monodisperse triangular or cubic NPs. Spherical NPs result only from the pre- cursors synthesized in the laboratory. The detailed Energy Dispersive X-ray spectrometry (EDS) and X-ray diffraction analysis performed on the commercial precursors (Commercial grade and washed) reveal the presence of impurities: sodium stearate and/or sodium chloride (NaCl). This result highlights the importance of iron stearate precursor origin (commercial grade or washed or home-made) in terms of reproducibility and growth of iron oXide NPs, giving rise to either monodisperse spherical, cubic, or triangular NPs. We emphasize that this finding majorly affects the development of NPs and also our understanding of the NP growth mechanisms, which can be biased if we do not account for this additional key parameter

among all the ones involved in the colloidal synthesis. The formation of the triangular nanoparticles in the conditions we use has never been reported. Further, the formation of both cubic and triangular NPs has been discussed in terms of selective adsorption on the growing NP of sodium stearate, sodium, and chloride salts.

KEYWORDS: Maghemite nanoparticles, thermal decomposition, iron stearate, impurities, cubic, triangular, and spherical shapes.

1. Introduction

In the last 20 years, iron oXide nanoparticles (NPs) have been extensively studied for their use in many technological applications such as energy storage [1], catalysis [2] and wastewater treatment [3]. In addition, thanks to their biocompatibility combined with their chemical stability, they are also widely used in biomedicine [4]. To continuously improve their performances, it is crucial to accu- rately control their structural characteristics (composition, nano crys- tallinity, size, geometry, and surface chemistry). Among the existing approaches to synthesizing NPs, the decomposition of metal precursors is more appropriate to favor uniform NPs. Using this strategy, uniform iron oXide NPs with controlled size [5–13] and shape [14–23] have been obtained. However, many key parameters must be controlled to suc- cessfully prepare well-defined populations. Hence, NP structural char- acteristics depend on the nature of the precursors, the ligands and the solvent, the heating rate, the reaction time, the reaction temperature, the precursor injection time, the surfactant to precursor ratio, and the presence of additives [24,25]. The reproducibility of these syntheses requires perfect control of all the key parameters playing a role in the formation of the NPs from the atomic scale (precursor decomposition, solvation of reactants, adsorp- tion of ligands and salts …) to the nanoscale (nucleation, growth, aging steps …). In addition, a deep understanding of the nucleation and growth mechanisms of NPs is crucial, especially to highlight novel nanomaterials. In this article, we report that one key parameter in the reproduc- ibility of spherical iron oXide NPs by the thermal decomposition of iron stearate precursor is its origin. In the literature, it has been reported that the use of iron stearate precursors from the supplier Strem Chemicals [11,12] leads to spherical iron oXide NPs. Here, we show that the same synthesis approach using commercial iron (II) and iron (III) precursors provided by Strem chemicals and TCI, respectively, yields different anisotropic shape NPs, i.e., triangular and cubic ones, with different sizes. Besides, a washing step performed for the iron (II) precursor (Strem chemicals), induces a change from triangular to cubic NPs. Finally, the spherical NPs are recovered by using a precursor synthesized in the laboratory. Thanks to a qualitative and quantitative chemical analysis study performed by energy dispersive X-ray spectrometry (EDS) analysis and X-ray diffraction (XRD), we evidence the presence of various impurities (sodium stearate and/or sodium chloride) in the two commercial precursors (used as-received or washed), explaining, the formation of anisotropic shape NPs. First, this study evidences the importance of the origin of the iron stearate precursor (as received commercially or washed, or homemade), i.e. its purity, on the growth of maghemite NPs as well as the role played by

the detected impurities on the determination of the particle shape (spherical, cubic and triangular). Second, it highlights that the identi- fication of the nature of the impurities, rarely proposed in the literature, is needed for the understanding of the NP growth mechanisms, which are still not totally elucidated. Third, the presence of the detected im- purities in the commercial precursors is explained in terms of mistakes made in their fabrication. Fourth, triangular NPs are here formed using a strategy, that has never been reported previously. In the last 20 years, iron oXide nanoparticles (NPs) have been extensively studied for their use in many technological applications such as energy storage [1], catalysis [2] and wastewater treatment [3]. In addition, thanks to their biocompatibility combined with their chemical stability, they are also widely used in biomedicine [4]. To continuously improve their performances, it is crucial to accu- rately control their structural characteristics (composition, nano crys- tallinity, size, geometry, and surface chemistry). Among the existing approaches to synthesizing NPs, the decomposition of metal precursors is more appropriate to favor uniform NPs. Using this strategy, uniform iron oXide NPs with controlled size [5–13] and shape [14–23] have been obtained. However, many key parameters must be controlled to suc- cessfully prepare well-defined populations. Hence, NP structural char- acteristics depend on the nature of the precursors, the ligands and the solvent, the heating rate, the reaction time, the reaction temperature, the precursor injection time, the surfactant to precursor ratio, and the presence of additives [24,25]. The reproducibility of these syntheses requires perfect control of all the key parameters playing a role in the formation of the NPs from the atomic scale (precursor decomposition, solvation of reactants, adsorp- tion of ligands and salts …) to the nanoscale (nucleation, growth, aging steps …). In addition, a deep understanding of the nucleation and growth mechanisms of NPs is crucial, especially to highlight novel nanomaterials. In this article, we report that one key parameter in the reproduc- ibility of spherical iron oxide NPs by the thermal decomposition of iron stearate precursor is its origin. In the literature, it has been reported that the use of iron stearate precursors from the supplier Strem Chemicals [11,12] leads to spherical iron oXide NPs. Here, we show that the same synthesis approach using commercial iron (II) and iron (III) precursors provided by Strem chemicals and TCI, respectively, yields different anisotropic shape NPs, i.e., triangular and cubic ones, with different sizes. Besides, a washing step performed for the iron (II) precursor (Strem chemicals), induces a change from triangular to cubic NPs. Finally, the spherical NPs are recovered by using a precursor synthesized in the laboratory. Thanks to a qualitative and quantitative chemical analysis study performed by energy dispersive X-ray spectrometry (EDS) analysis and X-ray diffraction (XRD), we evidence the presence of various impurities

(sodium stearate and/or sodium chloride) in the two commercial precursors (used as-received or washed), explaining, the formation of anisotropic shape NPs. First, this study evidences the importance of the origin of the iron stearate precursor (as received commercially or washed, or homemade), i.e. its purity, on the growth of maghemite NPs as well as the role played by the detected impurities on the determination of the particle shape (spherical, cubic and triangular). Second, it highlights that the identi- fication of the nature of the impurities, rarely proposed in the literature, is needed for the understanding of the NP growth mechanisms, which are still not totally elucidated. Third, the presence of the detected im- purities in the commercial precursors is explained in terms of mistakes made in their fabrication. Fourth, triangular NPs are here formed using a strategy, that has never been reported previously.

2. Experimental section

2.1. Chemicals

Iron (III) chloride ($FeCl_3.6H_2O$, 99%, VWR), sodium stearate ($CH_3(CH_2)_{16}COONa$, 97%, TCI), iron (II) stearate (9 % Fe, Strem Chemicals), iron (III) stearate (5.8 to 7% Fe, TCI), Oleic acid (99%, alpha aesar) and dioctyl ether (99%, sigma-aldrich).

2.2. Synthesis of iron (III) stearate precursor

Iron (III) stearate (FeSt3) was prepared by reaction of sodium stea- rate (NaSt) and iron (III) chloride salts (FeCl3) in an aqueous solution [13]. Sodium stearate (9.8 g, 32 mmol) is transferred into a two-necked round-bottomed flask (RBF) and solubilized in 320 mL of ultrapure water. The solution is heated to refluX at 120 ◦C and stirred for 30 min until complete dissolution of the stearate. Separately, FeCl3 (2.9 g, 10.7 mmol) is dissolved in 160 mL of ultrapure water and added to the so- dium stearate solution under vigorous stirring. A light orange precipitate formed immediately. The solution is kept under stirring at this tem- perature for 25 min. Thereafter the solution is allowed to cool to room temperature. The obtained precipitate is washed with 4 L of ultrapure water and filtrated with a Buchner funnel and oven-dried at 64 ◦C for 22h.

1.3. *Transmission Electron Microscopy (TEM)*

TEM study is performed using a JEOL JEM-1011 microscope at 100 kV. For this study, some drops of the colloidal solution are deposited on an amorphous carbon-coated TEM grid. The

average diameter and the polydispersity of NPs are determined from more than 500 NPs using ImageJ.

1.4. Microanalysis

The chemical compositions were determined by energy dispersive X-ray spectrometry (EDS) analysis using a scanning electron microscope (SEM, JEOL 5510 LV, Ltd, Tokyo, Japan) with IXRF Systems 500 digital processing.

1.5. X-ray diffraction

Powder X-ray diffraction (PXRD) diffractograms were recorded on a D8 DISCOVER of a Bruker XRD machine with a copper tube operating at 40 kV. All the samples were in the form of powder by which low background silicon sample holders were filled.

2.6. Synthesis of oleic acid coated γ-Fe_2O_3 nanoparticles

Synthesis of oleic acid-coated γ-Fe2O3 nanoparticles is based on the thermal decomposition approach reported in a previous study by Begin- Colin et al., [10,11] however some with slight modification i.e., a smaller volume of dioctyl ether (10 mL instead of 20 mL) and a higher heating rate (45 ◦C/min instead of 5 ◦C/min). 0.69 g (1.1 mmol) of iron (II) stearate (FeSt2) precursor (or 1 g (1.1 mmol) of iron (III) stearate (FeSt3) precursor), and 0.63 g (2.2 mmol) of

oleic acid are dissolved in 10 mL of dioctyl ether. This miXture is heated to the boiling point of dioctyl ether (287 ◦C) with a heating rate of 45 ◦C/ min, refluXed for 2 h, and then cooled to room temperature. A black solution is formed and washed with a large excess of acetone followed by centrifugation (4900 rpm, 5 min). The oleic acid-coated NPs are finally dispersed in chloroform. Five oleic acid-coated γ-Fe2O3 NP syntheses are performed with the same recipe described above with commercial iron (II) stearate pre- cursor from Strem Chemicals, as received (P_1), and washed (P_1^w), and iron (III) stearate precursor from TCI, as received (P_2) and washed (P_2^w), and iron (III) stearate precursor synthesized in the laboratory, (P_3). The commercial FeSt2 and FeSt3 precursors are washed as follows: 10 g of precursor in powder form is miXed with 150 mL of ultrapure water under vigorous stirring and is heated to 65 ◦C for 15 min. Then the mixture is cooled to room temperature. The precursor is then washed with 4 L of ultrapure water and filtrated with a Buchner funnel and oven- dried at 64 ◦C for 22 h.

3. Results and discussion

3.1. Synthesis of γ-Fe_2O_3 NPs using precursors P_1 and P_1^w

Fig. 1a and 1b show the TEM images of γ-Fe2O3 NPs synthesized using commercial grade iron (II) stearate (FeSt2), P_1. Low and high- magnification images reveal a population composed of almost uniform NPs with triangular shape. The corresponding size histogram (Fig. 1d), shows a mean triangle height and a size polydispersity of 9.7 nm and 16% respectively. Surprisingly, the synthesis performed with the same precursor but after being washed, P_1^w, leads to a single population of nanocubes. As shown in Fig. 1e and 1f, they are characterized by flat facets and sharp edges and their mean side diagonal is 10.5 nm. Thanks to a very low size polydispersity, 11% (Fig. 1h), they tend to self- organize in 2D superlattices.

3.1.1. Synthesis of γ-Fe_2O_3 NPs using precursor P_2 and P_2^w

Replacing iron (II) stearate (FeSt2) precursor P_1 with iron (III) stea- rate (FeSt3) precursor P2, while keeping other chemical components the same, results in a drastic change in the NP shape. Considering the as- received precursor (not washed), Fig. 1i and 1j clearly show that the population is made of nanocubes and not nanotriangles, which have rather similar characteristics compared to the sample prepared with the precursor P_1, i.e., a mean side diagonal and size polydispersity of 11.7 nm and 13% respectively (Fig. 1l). In this case, no washing effect on this precursor is observed as the population obtained with P_2^w, remains composed of nanocubes (Fig. 1m,1n) with similar mean side diagonal and size polydispersity of 11.7 nm and 11.7% respectively (Fig. 1p).

3.1.2. Synthesis of γ-Fe_2O_3 NPs using precursor P_3

Finally, using a precursor we synthesized in the laboratory iron (III) stearate (FeSt3), P_3, a single population of spherical γ-Fe2O3 NPs form (Fig. 1q, 1r). The size histogram (Fig. 1t) shows a mean diameter of 6.7 nm with a size polydispersity of 12%. From previous studies reported in the literature [9–13], a similar approach used to synthesize maghemite NPs induces the formation of spherical ones. In our study, we find that spherical NPs are only formed with the use of the home-made precursor P_3 and never with the com- mercial ones (as-received and washed). In addition, our results clearly evidence a drastic impact of both the supplier and the washing of the commercial product in the anisotropic shape of NPs. To understand this puzzling result, elemental analysis and X-ray diffraction studies have been performed for the different precursors to determine the possible impurities

qualitatively and quantitatively, which could explain the differences we observe in the NP growth that in turn their final shape.

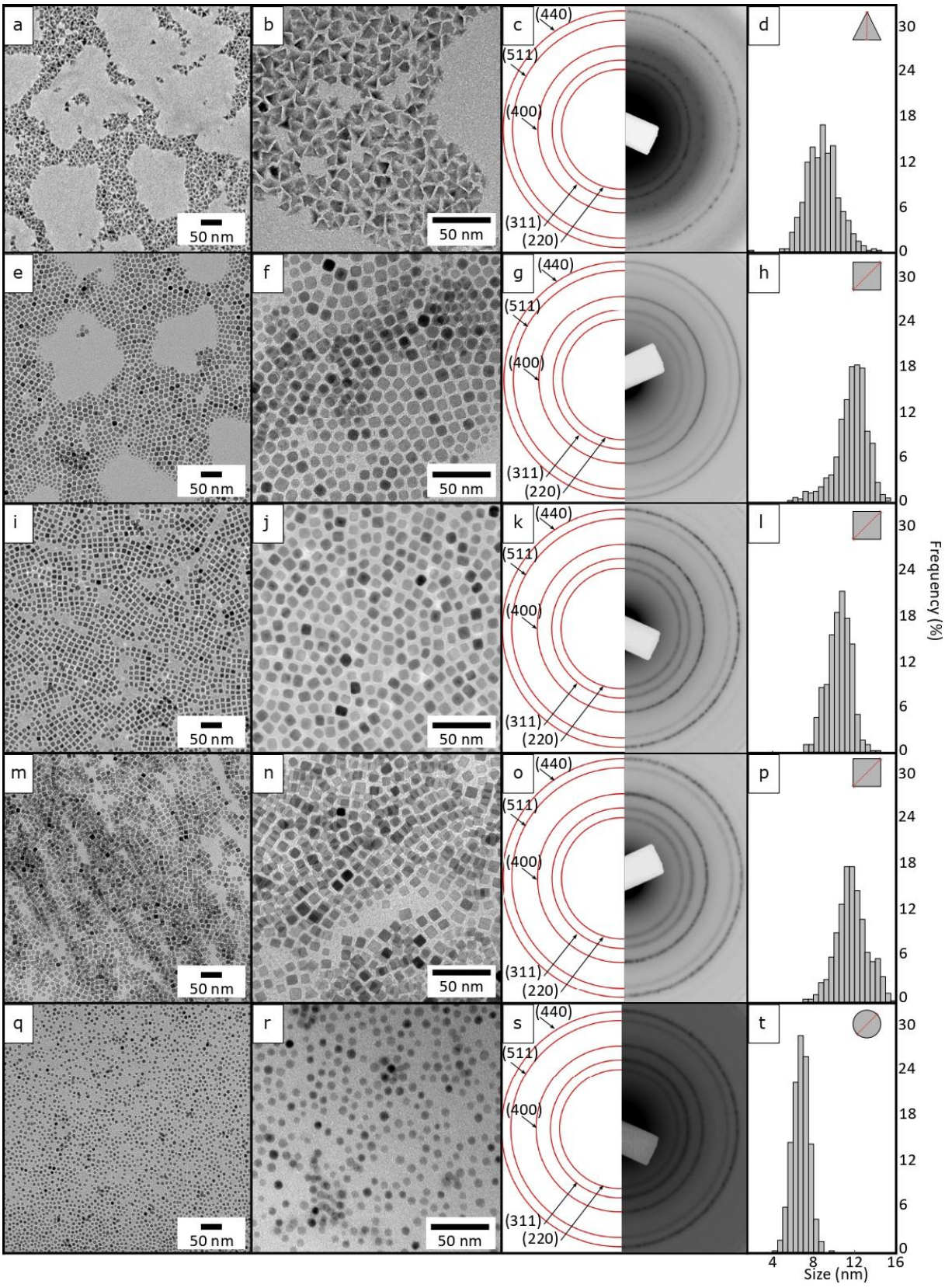

Fig. 1. TEM images, corresponding electron diffraction patterns, and size histograms of maghemite (γ-Fe2O3) nanoparticles synthesized with P_1 (a,b,c,d), P_1^w (e,f,g,h),

P_2 (i,j,k,l), P_2^w (m,n,o,p) and P_3 (q,r,s,t) precursors.

3.2. Study of the crystalline structure of the nanoparticles

3.2.1 Electron diffraction

The crystalline structure of the five populations of NPs obtained with P_1, P_2, P_1^w, and P_2^w and P_3 precursors have been investigated by the selected area (electron) diffraction (SAED). Whatever the precursor used and the shape of the NPs are, the electron diffraction patterns (Figs. 1c, 1g, 1k, 1o,1s) show five rather thin diffraction rings at 1.47, 1.60, 2.08, 1.51, and 2.95 Å corresponding to the (440), (511), (400), (311), and (220) planes of a maghemite iron oxide phase according to the JCPD 39-1346 database. However, it's important to note that the lattice spacings of the maghemite and magnetite phases are very close. This is thus difficult to conclude that our samples consist of pure maghemite. To address this uncertainty, we use the X-ray diffraction technique to gain a more comprehensive understanding of the crystal structures of our NPs.

3.2.2 X-ray diffraction

To discriminate between magnetite and maghemite phases of the iron oxide nanoparticles synthesized by using the different precursors (P_1^w, P_2, P_2^w, P_3), we follow the method developed by Kim et al. [26] based on the X-ray analysis. The X-ray corresponding patterns are presented in Fig. 2. For all the samples, we detect the peaks characteristic of maghemite or magnetite, i.e., while peaks corresponding to hematite and wüstite are noticeably absent. The two peaks (210) and (211), which are the signature of exclusive maghemite are observed for the spherical and cubic NPs obtained with the precursors P_3 and P_2^W respectively. The cubic NPs synthesized with P_2 precursor show the (210) peak but not the (211) peak while the cubic NPs obtained with the P_1^w show the opposite trend. The presence of the (210) and/or (211) peaks, coexisting with the others ((220), (311), (400), (422), (511), (440)), is indicative of either pure maghemite or a mixture of maghemite and magnetite. However, as reported by Kim et al. [26], the position of the peak (511) is essential as it allows to discriminate between magnetite

and maghemite phases. Indeed, they show that the (511) peak shifts from 57◦ to 57.3◦ from pure magnetite to pure maghemite phase. In the case of a combination of both phases, they observe a larger peak, with a shoulder, composed of the lower and the higher angle peak [26]. As shown in the inset of Fig. 2, which represents the magnified regions between 50◦ and 60◦ of the diffraction patterns, all the (511) peaks are found at a value 2 Theta of 57.3◦ and appear symmetric. No shoulder characteristic of a mixture of maghemite and magnetite is observed. This feature, which agrees with the presence of the (210) and/or (211) peaks, allows us to conclude the formation of pure maghemite NPs for the spherical and cubic NPs obtained with the P_1^w, P_2, P_2^w, and P_3 precursors. Unfortunately, the triangular colloidal NP solution obtained with the P_1 precursor, could not be studied by XRD. This is explained by the too-low concentration of the colloidal solution. Indeed, we noticed that the triangular NP powder appears light red, in contrast to the black color of the other shape samples. This color variation is attributed to the presence of the precursor (color and texture). The low concentration of this

population is explained by the low yield of this thermal decomposition reaction. However, the electron diffraction signature of the triangle NPs is like that of the spherical and cubic NPs. This permits us to conclude the formation of maghemite triangular NPs. In summary, thanks to a comprehensive structural study with both electron and/or X-ray diffraction techniques, we conclude the formation of pure maghemite for the spherical, cubic, and triangular NPs synthesized with the P_1, P_1^w, P_2, P_2^w, and P_3 precursors. This result evidences that the impurities involved in the reaction, through the precursor, do not impact the crystalline structure of the iron oxide NPs. Conversely, it has a drastic effect on NP growth and therefore on the final shapes.

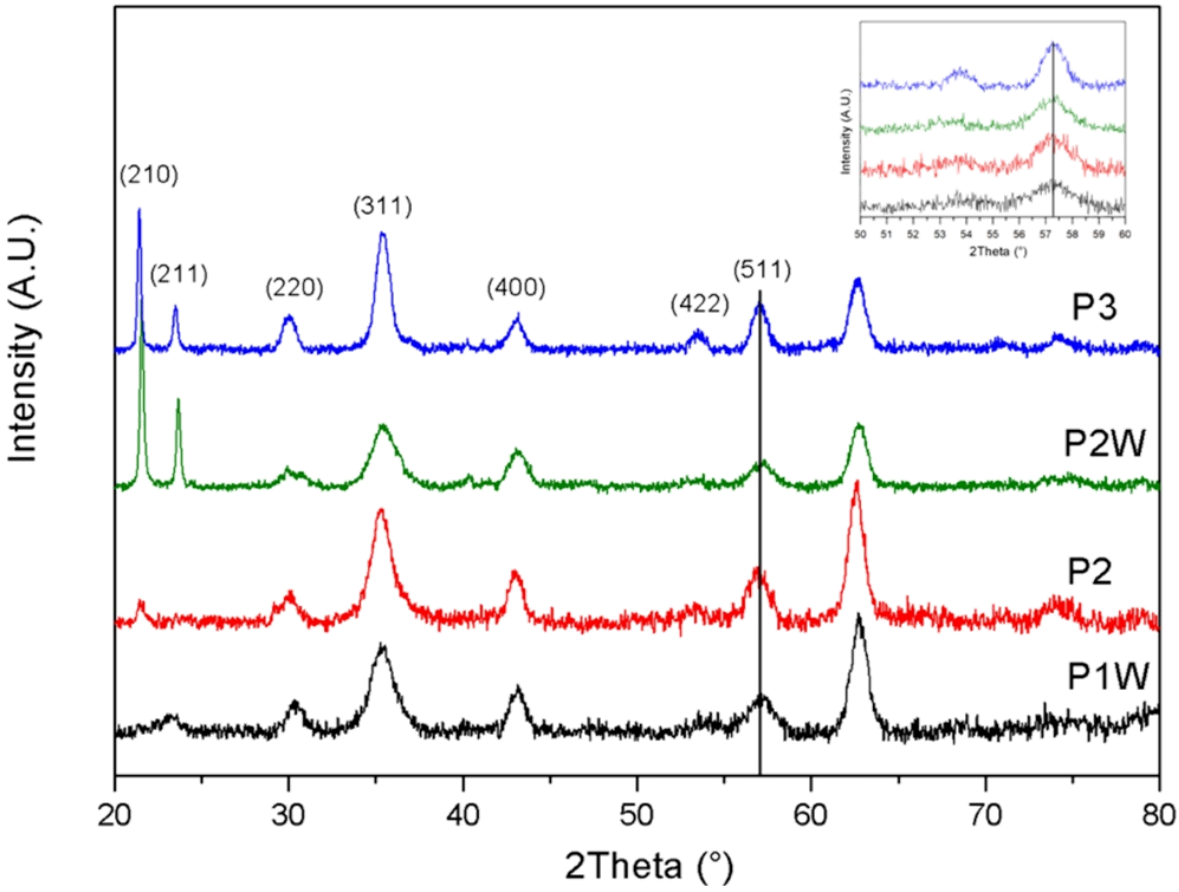

Fig. 2. XRD patterns of nanoparticles synthesized with P_1^w, P_2, P_2^w, and P_3 (e) precursors. Inset: magnified regions between 50◦ and 60◦ of the diffraction patterns.

3.3. Characterization of P_1, P_2, P_1^w and P_2^w and P_3 precursors

3.3.1. Elemental analysis study on P_1, P_2, P_1^w and P_2^w and P_3 precursors

Elemental analysis spectra performed for the five precursors are shown in Fig. 3. In addition to the iron, and while not expected, sodium and chlorine elements are detected for the commercial precursors. The relative atomic composition of the three elements obtained by quantification of the spectra is reported in Table 1. If we focus on the precursor P_1 from Strem Chemicals, it appears that it contains a high atomic percent of sodium elements, 48%. After its washing, (P_1^w), this value remains almost unchanged, 49%. Besides, 27% of chloride is detected on the as-received precursor while this value drops to 3% after its washing (P_1^w). Concerning the TCI commercial precursor, P_2, it also contains a high atomic percent of sodium elements, 34%, however only 14% of chloride is detected. P_2 washing mainly induces

the drop of this last value to 4%. The same analysis performed on the home-made precursor (P_3) clearly shows that neither sodium nor chloride are detected.

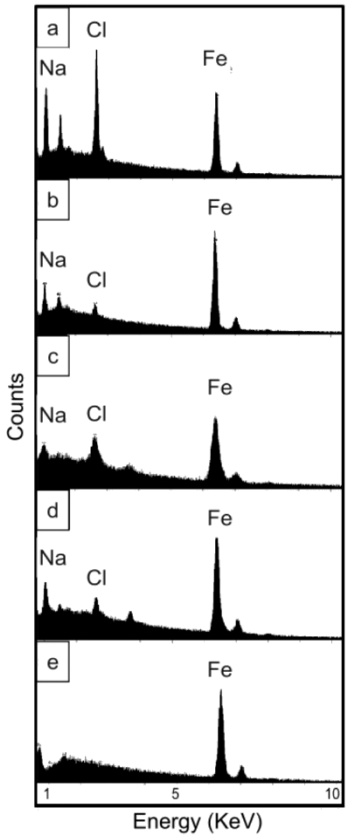

Fig. 3. EDX patterns of P_1 (a), P_1^w (b), P_2 (c), P_2^w (d), and P_3 (e) precursors

Table 1: Relative atomic percentage of Fe, Na and Cl of the *P1*, *P1w*, *P2*, *P2w* and *P3* precursors.

Precursor	***Atom%***		
	Fe	**Na**	**Cl**
P_1	**25**	**48**	**27**
P_1^w	**48**	**49**	**3**
P_2	**52**	**34**	**14**
P_2^w	**58**	**38**	**4**
P_3	**100**	**0**	**0**

3.3.2. X-ray diffraction study on P_1, P_2, P_1^w, P_2^w and P_3 precursors

To determine, the nature of the compounds present in the commercial P_1, P_2, P_1^w *and* P_2^w precursors, an X-ray diffraction study has been performed. The XRD diffractograms are shown in Fig. 4. For P_1 and P_2 precursors, one can detect two peaks at 31.7◦, and 45.5◦ (marked with *) corresponding to the (200) and (220) plane reflections respectively, of NaCl salt [27]. After their washing, (P_1^w, P_2^w), these peaks are not anymore observed. If we focus on the smaller angle diffraction pattern, and for all the commercial precursors, P_1, P_2, P_1^w *and* P_2^w, one intense peak at around 22◦ (marked with ◦) is observed. This peak is attributed to NaSt [28]. The XRD pattern of the home-made precursor (P_3) is characteristic of the pure lamellar structure Fe(St)3 without any evidence of the presence of neither NaCl nor NaSt. This XRD study is in good agreement with the elemental analysis. The presence of NaCl and NaSt is evidenced in the two as-received commercial precursors. After their washing, NaCl salt disappears. Finally, the home-made precursor is characterized by pure FeSt3.

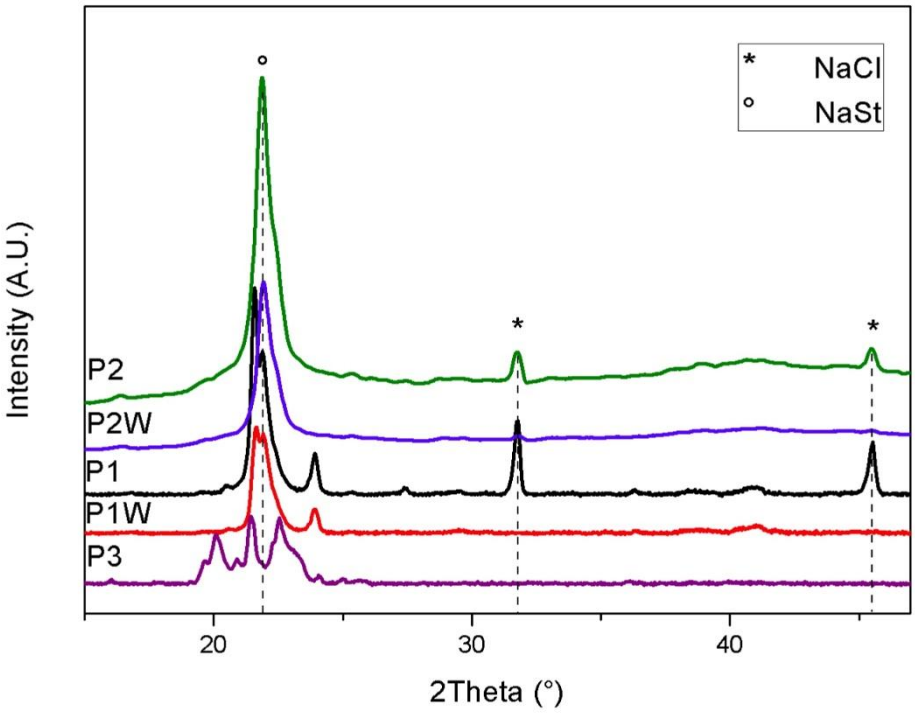

Fig. 4. XRD patterns of P_1, P_1^w, P_2, P_2^w, and P_3 precursors.

3.4. How to explain the presence of the detected impurities in the commercial precursors?

The results obtained by chemical and XRD analyses are interpreted as the following. The home-made precursor, P_3, has been synthesized in the stoichiometric conditions of the reaction:

$$FeCl_3 + 3\ NaSt \Rightarrow FeSt_3 + 3NaCl$$

i.e., 3 sodium stearate for 1 iron chloride (*see experimental section*). Once the iron precursor is obtained, the solution is washed with a large amount of ultrapure water (4L) to remove the totality of the amount of sodium and chloride ions by-products. Considering the chemical analysis (Table 1), the absence of detection of these two by-products confirms that the iron precursor P_3 obtained is pure. Conversely, for the as-received (not washed) commercial precursor P_1, a large amount of sodium and chloride ions are detected (Table 1). In addition, we note that the amount of sodium (48 %) is higher compared to that of chloride ions (27%). This result makes us suggest that first, P_1 synthesis has not been performed in the stoichiometric conditions of the reaction but with a ratio of the sodium stearate to the chloride iron concentration higher than 3, leading to the presence of remaining sodium stearate and sodium chloride as by-products. Second, the washing step of the solution has not been optimal, otherwise, chloride ions would not be present. Our explanation is confirmed through the analysis of the precursor after its washing with 4L of ultrapure water (P_1^w). The amount of detected chloride drops from 27 to 3 %, while that of sodium ions remains high (49 %) (Table 1). Conversely to the chloride ions, sodium ions cannot be removed during the washing with water as it forms the sodium stearate complex, which is not soluble in water. So, one can conclude that P_1^w precursor contains a mixture of iron and sodium stearate in almost equal concentration. For the as-received commercial precursor P_2 (not washed), sodium (34 %) and chloride (14 %) are also detected. (Table 1). After its washing, the amount of chloride drops to 4 %. Similar findings as for P_1 apply. However, the lower amount of sodium and chloride compared to P_1 suggests that P_2 has been produced in closer stoichiometric conditions compared to the synthesis of P_1.

3.5. Interpretation of the γ-Fe_2O_3 nanoparticle shape, in light of the nature of the impurities detected in the commercial iron stearate precursors

In light of the chemical and XRD analyses, the variety of maghemite NP shapes obtained can only be explained in terms of the purity of the iron precursors. All the other synthesis conditions are equal (ligand, solvent, heating rate, temperature, and reflux time).

When the synthesis is performed with the home-made iron stearate precursor (pure), oleic acid plays the role of universal stabilizer on each facet of the NPs, and the final NPs are spherical. In the literature, this behavior is well illustrated in several papers [10, 11] reporting the formation of spherical iron oxide NPs by the thermal decomposition of iron stearate in the presence of oleic acid, without any additives. Begin-Colin et al. have evidenced that, regardless of the number of stearate chains of the iron precursor, $FeSt_2$ or $FeSt_3$ leads to spherical NPs [13, 29]. It is noteworthy that spherical iron oxide NPs have also been obtained with oleate precursors, always in the presence of oleic acid and without any additives [6, 8].

Conversely, when additives are present in the reaction medium, anisotropic NP growth can occur, resulting from their selective adsorption on the NP facets. For example, the addition of sodium oleate is expected to lead to cubic iron oxide NPs [14, 18, 21, 30, 31]. In this case, nanocubes are induced by the selective adsorption of the sodium oleate on the {100} facets of iron oxide. This induces the faster growth of the NP along the [111] direction over the [100] leading to surfaces composed of {100} facets. Comparative studies show, without any ambiguity, that the same approach performed in the absence and ~~in~~ the presence of sodium oleate, gives rise to spherical and cubic NPs respectively [14, 31]. Therefore, one can conclude that cubic NP growth formed by using the commercial precursors (P_1^w, P_2, and P_2^w), could be determined by the key role played by the sodium stearate.

The formation of the triangular NPs (tetrahedral geometry), is more puzzling. Chemical analysis indicates that the precursor P_1, yielding this shape, contains both sodium stearate and NaCl salt. Sodium stearate, here, is expected to bind to the {100} facets of iron oxide to form cubic NPs and then, does not seem to play a role in the formation of triangular NPs. However, it has been reported by Kovalenko et al. [14] that the thermal decomposition of iron oleate in the presence of sodium oleate gives rise to either nanocubes or a mixture of nanocubes and bipyramidal NPs. The first ones are obtained with a $NaOL/Fe(OL)_3$ molar ratio of 1 and a heating rate of 3.3°C/min. The second ones are formed using similar growth conditions as for cubes, but by decreasing the $NaOL/Fe(OL)_3$ molar ratio to 0.67 and by reducing the heating rate to 1°C/min. Besides, using the same approach with iron oleate precursor and sodium oleate ligand, Zhou et al. [21] observed, in mild conditions (with octadecene as solvent), the formation of Fe_3O_4 {111} facet exposed tetrahedrons, while in a higher boiling temperature

solvent (tri-n-octylamine), they form nanocubes. These two examples indicate that sodium oleate may play various roles in different conditions. Concerning our study, the question is "Does the presence of NaCl in the commercial precursor P_1, could favor such a versatility of the role of sodium stearate?" At this moment, this question remains open. Otherwise, another question arises regarding the role played by Cl^- or Na^+ ions, in excess in the precursor P_1. Gao et al. [32] have shown that Cl^- adsorbs on the {100} facets of magnetite-yielding nanocubes. If we focus on the tetrahedral geometry, one hypothesis is that Na^+ ions selectively adsorb on the {111} facets of maghemite. This strategy is not excluded in a previous study reported by Liz-Marzan [31]. Besides, in a previous study performed in the laboratory, the use of Cl^- and Br^- ions has been shown to control the shape of copper NPs from nanorods to nanocubes [33]. Therefore, it is reasonable to think that either sodium stearate and/or Na^+, Cl^- ions, could be the key parameters in the growth of the triangular maghemite NPs.

3.6. Does the nature of the precursor, $FeSt_2$ and $FeSt_3$ play a role in the growth of cubic and triangular maghemite nanoparticles?

In recent papers, Begin-Colin et al. has reported the role played by the number of stearate chains (2 and 3) of the iron stearate precursors on the growth of iron oxide nanoparticles [13, 29, 34 and 35]. They have studied the influence of the ratio sodium oleate (NaOL) / oleic acid (OA) with $FeSt_2$ and $FeSt_3$ iron stearate precursors differing by their hydration state, on the shape of nanoparticles. The authors demonstrate clearly, the important role played by the presence of NaOL on the NP shape. Nanospheres are obtained in the absence of NaOL, i.e., with only OA**.** Facetted shapes are obtained, when NaOL is added, even at low concentration. They also show that the evolution of the shape with the amount of NaOL can depend on the nature of the precursor, $FeSt_2$ and $FeSt_3$, and on their hydration degree. For the NaOL/OA ratio (20/80), less-rounded NPs are obtained for all precursors. When this ratio increases, $FeSt_2$ and dehydrated $FeSt_2$ are allowed to obtain nanoplates while $FeSt_3$ and dehydrated $FeSt_3$ lead to nanocubes. The change in the NP shape is explained in terms of the thermal stability of the precursors, which differs from $FeSt_2$ to $FeSt_3$ iron stearate precursors.

In our study, we evidence that *maghemite nanocubes* are obtained with both $FeSt_2$ washed (P_1^w) and $FeSt_3$ washed and not washed (P_2^w, P_2) precursors. In addition, for all three cases, we identify a constant environment, i.e., the presence of sodium stearate, which is known to drive the nanoparticle growth toward cubic shape (*see &3.4*). This result thus does not allow us to conclude an effect of the nature of the stearate precursor on the NP shape. However, it

evidences the crucial role played by the presence of sodium stearate in the formation of maghemite nanocubes.

Focusing on the *triangular maghemite NPs*, we show in this paper that they are obtained with $FeSt_2$ not washed (P_1) precursor in the presence of NaSt, $Na^{+,}$ and Cl^- ions. However, the same precursor, $FeSt_2$ washed (P_1w) leads to nanocube growth. In addition, the triangular NPs are only obtained in the presence of NaSt, $Na^{+,}$ and Cl^- while the nanocubes are obtained in the presence of NaSt. This behavior makes us conclude with the importance of the "impurities" in the formation of the triangles rather than the role played by the nature of the precursor.

Therefore, from the study presented in this paper, a possible impact of the nature of the precursor on the growth of anisotropic shape NPs cannot be evidenced.

This study clearly shows that the supplier, i.e. the purity of the iron stearate, must be taken into account in the reproducibility of maghemite NP syntheses. This ~~clearly~~ constitutes another key parameter in the formation of NPs. Such finding has already been reported for other colloidal syntheses for example [36] and constitutes an impediment to the development of NPs as well as to the understanding of the growth mechanisms involved in these syntheses.

CONCLUSION

In the literature, the thermal decomposition of commercial iron stearate precursor in the presence of oleic acid surfactant (in the absence of additives) yields spherical iron oxide NPs. We show that the use of similar commercial iron precursors (used with and without a washing step) does not yield any more to the spherical but to a uniform and single

population of cubic or triangular maghemite NPs. The presence of "impurities" identified as NaSt and NaCl by accurate chemical analysis and XRD study made on these precursors allow (1) to explain the cubic NP growth and (2) to highlight a new route to synthesize triangular maghemite NPs. Very few studies have been reported in the literature regarding triangular iron oxide NPs, whose growth remains unexplored. However, for highlighting novel magnetic properties, these NPs are very interesting. Further work will focus on the study of their formation mechanism to accurately control their structural properties and explore their magnetic properties.

ACKNOWLEDGEMENTS: Authors thank (1) the “Institut de Sciences des Mat´eriaux " (IMAT) of the ”Alliance Sorbonne Universit´e ”, "Investigation of nanoparticle size effect on the properties of nano-reinforced polymers ", contract number IMAT – DOCTORANT SORBR122RRO, and (2) the ANR NanoHype " Temperature Profile in Nanomagnet based Hyperthermia Devices", contract number ANR-21-CE09–0043, for supporting this work. Thanks are also due to Mr Baptiste Roselli from the MONARIS laboratory (France) for his help with the X-ray diffraction measurements.
Thanks are also due to Mr Baptiste Roselli from the MONARIS laboratory (France) for his help with the X-ray diffraction measurements.

REFERENCES

[1] S. Sheng, W. Liu, K.Zhu, K. Cheng, K. Ye, G.Wang, D. Cao, J. Yan, Fe_3O_4 nanospheres in situ decorated graphene as high-performance anode for asymmetric supercapacitor with impressive energy density, Journal of colloid and interface science 536 (2019) 235-244.

[2] Z.S. Wu, S. Yang, Y. Sun, K. Parvez, X. Feng, K. Müllen, 3D nitrogen-doped graphene aerogel-supported Fe_3O_4 nanoparticles as efficient electrocatalysts for the oxygen reduction reaction, Journal of the American Chemical Society 134, no. 22 (2012) 9082-9085.

[3] S. Liu, B.Yu, S.Wang, Y. Shen, H. Cong, Preparation, surface functionalization and application of Fe_3O_4 magnetic nanoparticles, Advances in colloid and Interface Science 281 (2020) 102165.

[4] C. Blanco-Andujar, A. Walter, G. Cotin, C. Bordeianu, D. Mertz, D. Felder-Flesch, S. Begin-Colin, Design of iron oxide-based nanoparticles for MRI and magnetic hyperthermia, Nanomedicine 11, no. 14 (2016) 1889-1910.

[5] S. Sun, Shouheng, H. Zeng, Size-controlled synthesis of magnetite nanoparticles, Journal of the American Chemical Society 124, no. 28 (2002) 8204-8205.

[6] N.R. Jana, Y. Chen, X. Peng, Size-and shape-controlled magnetic (Cr, Mn, Fe, Co, Ni) oxide nanocrystals via a simple and general approach, Chemistry of materials 16, no. 20 (2004) 3931-3935.

[7] F.X. Redl, C. T. Black, G.C. Papaefthymiou, R.L. Sandstrom, M. Yin, H. Zeng, C.B. Murray, S.P. O'Brien, Magnetic, electronic, and structural characterization of nonstoichiometric iron oxides at the nanoscale, Journal of the American Chemical Society 126, no. 44 (2004) 14583-14599.

[8] J. Park, K. An, Y. Hwang, J.G. Park, H.J. Noh, J.Y. Kim, J.H. Park, N.M. Hwang,T. Hyeon., Ultra-large-scale syntheses of monodisperse nanocrystals, Nature materials 3, no. 12 (2004) 891-895.

[9] A. Demortiere, P. Panissod, B. Pichon, D. Pourroy, D. Guillon, B. Donnio, S. B´egin-Colin, Size-dependent properties of magnetic iron oxide nanocrystals, Nanoscale 3 (1) (2011) 225–232.

[10] M. Pauly, B. Pichon, P. Panissod, S. Fleutot, P. Rodriguez, M. Drillon, S. Begin-Colin, Size dependent dipolar interactions in iron oxide nanoparticle monolayer and multilayer Langmuir–Blodgett films, Journal of Materials Chemistry 22, no. 13 (2012) 6343-6350.

[11] W. Baaziz, B. Pichon, S. Fleutot, Y. Liu, C. Lefevre, J. M.Greneche, M. Toumi, T. Mhiri, S. Begin-Colin, Magnetic iron oxide nanoparticles: reproducible tuning of the size and

nanosized-dependent composition, defects, and spin canting, The Journal of Physical Chemistry C 118, no. 7 (2014) 3795-3810.

[12] W. Baaziz, B. P. Pichon, J.M. Grenèche, S. Begin-Colin, Effect of reaction environment and in situ formation of the precursor on the composition and shape of iron oxide nanoparticles synthesized by the thermal decomposition method, CrystEngComm 20, no. 44 (2018): 7206-7220.

[13] G. Cotin, C. Kiefer, F. Perton, M. Boero, B. Ozdamar, A. Bouzid, G.Ori, C. Massobrio, D. Begin, B. Pichon, D. Mertz, S. Begin-Colin, Evaluating the critical roles of precursor nature and water content when tailoring magnetic nanoparticles for specific applications, ACS Applied Nano Materials 1, no. 8 (2018) 4306-4316.

[14] M.V. Kovalenko, M.I. Bodnarchuk, R.T. Lechner, G. Hesser, F. Schäffler, W. Heiss, Fatty acid salts as stabilizers in size-and shape-controlled nanocrystal synthesis: the case of inverse spinel iron oxide, Journal of the American Chemical Society 129, no. 20 (2007) 6352-6353.

[15] H. Yang, T. Ogawa, D. Hasegawa, M. Takahashi, Synthesis and magnetic properties of monodisperse magnetite nanocubes, Journal of Applied Physics 103, no. 7 (2008) 07D526.

[16] D. Kim, N. Lee, M. Park, B.H. Kim, K. An, T. Hyeon, Synthesis of uniform ferrimagnetic magnetite nanocubes, Journal of the American Chemical Society 131, no. 2 (2009) 454-455.

[17] P. Guardia, N. Pérez, A. Labarta, X. Batlle, Controlled synthesis of iron oxide nanoparticles over a wide size range, Langmuir, 26 (2010)5843–5847.

[18] M. Pauly, B. Pichon, P. Albouy, S. Fleutot, C. Leuvrey, M. Trassin, J.L. Gallania S. Begin-Colin, Monolayer and multilayer assemblies of spherically and cubic-shaped iron oxide nanoparticles, J. Mater. Chem, 21 (2011) 16018–16027.

[19] L.H. Zhang, J.J. Wu, H.B. Liao, Y.L. Hou, S. Gao, Octahedral Fe_3O_4 nanoparticles and their assembled structures. Commun, 29 (2009) 4378–4380.

[20] Z. Zhao, Z. Zhou, J. Bao, Z. Wan, J. Hu, X. Chi, K. Ni, R. Wang, X. Chen, Z. Chen, J. Gao, Octapod iron oxide nanoparticles as high-performance T2 contrast agents for magnetic

[21]- Zhou, Z.; Zhu, X.; Wu, D.; Chen, Q.; Huang, D.; Sun, C.; Xin, J.; Ni, K.; Gao, J.; Anisotropic shaped iron oxide nanostructures: controlled synthesis and proton relaxation shortening effects. Chem. Mater. (2015), 27, 3505–3515.

[22] A.G. Roca, L. Gutiérrez, H. Gavilán, M.E. Fortes Brollo, S. Veintemillas-Verdaguer, M. del Puerto Morales, Design strategies for shape-controlled magnetic iron oxide nanoparticles, Advanced Drug Delivery Reviews, 138 (2019) 68–104.

[23] M.D. Nguyen, H.V. Tran, S. Xu, T.R. Lee, Fe_3O_4 nanoparticles: structures, synthesis, magnetic properties, surface functionalization, and emerging applications, Appl. Sci. 11 (2021) 11301.

[24] J. Park, J. Joo, S.G. Kwon, Y. Jang, T. Hyeon, Synthesis of Monodisperse Spherical Nanocrystals. Angew. Chem. 46 (2007) 4630-4660.

[25] L. Wu, A. Mendoza-Garcia, Q. Li, S. Sun, Organic Phase Syntheses of Magnetic Nanoparticles and Their Applications, Chem. Rev. 116 (2016) 10473−10512.

[26] W. Kim, C.Y Suh, S.W Cho, K.M Roh, H Kwon, K Song, I.J Shon, A new method for the identification and quantification of magnetite-maghemite mixture using conventional X-ray diffraction technique.

[27] M. Rabiei, A. Pelevicius, A. Dashti, S.Nasiri, A. Monshi, A. Vilkauskas, G. Janusas, Measurement Modulus of elasticity related to the atomic density of planes in unit cell of crystal lattices, Materials 13 issue 19 (2020) 4380.

[28] J. Liang, Y. Ma, Y. Zheng, H.T. Davis, Solvent-induced crystal morphology transformation in a ternary soap system: sodium stearate crystalline fibers and platelets, Langmuir 17 issue 21 (2001) 6447-6454.

[29] F. Perton, G. Cotin, C. Kiefer, J.M. Strub, S. Cianferani, J.M. Greneche, N. Parizel, B. Heinrich, B. Pichon, D. Mertz, S. Begin-Colin, Iron Stearate Structures: An Original Tool for Nanoparticles Design, Inorg. Chem, 60 (2021) 12445-12456.

[30] A. Shavel, B. Rodríguez-González, M. Spasova, M. Farle, L.M. Liz-Marzán, Synthesis and Characterization of Iron/Iron Oxide Core/Shell Nanocubes, Adv. Funct. Mater. 17 (2007) 3870-3876.

[31] A. Shavel, L.M. Liz-Marzán, Shape control of iron oxide nanoparticles. Phys. Chem. Chem. Phys. 11 (2009) 3762–3766.

[32]Z. Xu, C. Shen, Y. Tian, X. Shi, H.J. Gao, Organic phase synthesis of monodisperse iron oxide nanocrystals using iron chloride as precursor, Nanoscale, 2 (2010) 1027–1032.

[33] A. Filankembo, S. Giorgio, I. Lisiecki, M.P. Pileni, Is the anion the major parameter in the shape control of nanocrystals?, J. Phys. Chem. B. 107,(2003) 7492-7500.

[34] G. Cotin, C. Kiefer, F. Perton, D. Ihiawakrim, C.Blanco-Andujar, S. Moldovan, C. Lefevre, O. Ersen, B. Pichon, D. Mertz, S. Begin-Colin, Unravelling the Thermal Decomposition Parameters for The Synthesis of Anisotropic Iron Oxide Nanoparticles, ACS Applied Nano Materials 8 (2018) 881.

[35] G. Cotin, F. Perton, C. Petit, S. Sall, C. Kiefer, V. Begin, B. Pichon, C. Lefevre, D. Mertz, J.M. Greneche, S. Begin-Colin, Chem. Mat, 32 (2020) 9245-9259.

[36] D.K. Smith, B.A. Korgel, The Importance of the CTAB Surfactant on the Colloidal Seed-Mediated Synthesis of Gold Nanorods, Langmuir 24 (2008) 644-649.